

1
2
3
4
5
6
7
8
9
10
11
12
13
14
15
16
17
18
19
20
21
22
23
24

Lysosomal proteases are a determinant of coronavirus tropism

Yuan Zheng ^{1, #}, Jian Shang ^{1, #}, Yang Yang ^{1, #}, Chang Liu ¹, Yushun Wan ¹,
Qibin Geng ¹, Michelle Wang ¹, Ralph Baric ², Fang Li ^{1, *}

¹ Department of Veterinary and Biomedical Sciences, College of Veterinary Medicine,
University of Minnesota, Saint Paul, MN 55108, USA

² Department of Epidemiology, University of North Carolina, Chapel Hill, NC 27559,
USA

#These authors contributed equally to this work.

* Correspondence: Fang Li (lifang@umn.edu)

Running title: Coronavirus tropism and lysosomal proteases

Key words: coronavirus spike protein, lysosomal proteases, species tropism, tissue
tropism

25 **Abstract**

26 Cell entry of coronaviruses involves two principal steps: receptor binding and
27 membrane fusion, the latter of which requires activation by host proteases, particularly
28 lysosomal proteases. Despite the importance of lysosomal proteases in both coronavirus
29 entry and cell metabolism, the correlation between lysosomal proteases and cell tropisms
30 of coronaviruses has not been critically established. Here we examined the roles of
31 lysosomal proteases in activating coronavirus-surface spike proteins for membrane
32 fusion, using the spike proteins from SARS and MERS coronaviruses as the model
33 system. To this end, we controlled the contributions from receptor binding and other host
34 proteases, thereby attributing coronavirus entry solely or mainly to the efficiency of
35 lysosomal proteases in activating coronavirus-spike-mediated membrane fusion. Our
36 results showed that lysosomal proteases from bat cells support coronavirus-spike-
37 mediated pseudovirus entry and cell-cell fusion more effectively than their counterparts
38 from human cells. Moreover, purified lysosomal extracts from bat cells cleave cell-
39 surface-expressed coronavirus spike proteins more efficiently than their counterparts
40 from human cells. Overall, our study suggests that differential lysosomal protease
41 activities from different host species and tissue cells are an important determinant of the
42 species and tissue tropism of coronaviruses.

43

44

45

46 **Significance**

47 Coronaviruses are capable of colonizing new species, as evidenced by the recent
48 emergence of SARS and MERS coronaviruses; they can also infect multiple tissues in the
49 same species. Lysosomal proteases play critical roles in coronavirus entry by cleaving
50 coronavirus-surface spike proteins and activating the fusion of host and viral membranes;
51 they also play critical roles in cell physiology by processing cellular products. How do
52 differential lysosomal protease activities from different cells impact coronavirus entry?
53 Here we controlled the contributions from known factors that function in coronavirus
54 entry, such that lysosomal protease activities became the only or main determinant of
55 coronavirus entry. Using pseudovirus entry, cell-cell fusion, and biochemical assays, we
56 showed that lysosomal proteases from bat cells activate coronavirus-spike-mediated
57 membrane fusion more efficiently than their counterparts from human cells. Our study
58 provides the first direct evidence supporting lysosomal proteases as a determinant of the
59 species and tissue tropism of coronaviruses.
60

61 **Introduction**

62 One of the most outstanding features of viruses is their tropism, including species
63 and tissue tropism (1). Viral entry into host cells is among the most important
64 determinants of viral tropism (2-4). Entry of enveloped viruses involves two steps:
65 receptor binding and membrane fusion. Enveloped viruses often hijack the endocytosis
66 pathway: they enter endosomes, proceed to lysosomes, and then fuse the viral and
67 lysosomal membranes. The lysosomes play critical roles in cell metabolism by breaking
68 down biomolecules and cellular debris and also by providing nutrients for other cellular
69 functions (5, 6). The lysosomal protease activities are central to the functions of
70 lysosomes (7). They are also required to activate the membrane fusion of a variety of
71 viruses including coronaviruses and filoviruses (8-11). Understanding the correlation
72 between lysosomal protease activities and viral tropism has important implications for
73 investigating viral pathogenesis, developing antiviral strategy, and identifying zoonotic
74 strains with prepandemic potential.

75 Coronaviruses are large, enveloped, and single-stranded RNA viruses (12, 13).
76 They pose significant health threat to humans and other animals. Severe acute respiratory
77 syndrome coronavirus (SARS-CoV) was responsible for the SARS epidemic in 2002-
78 2003, causing over 8000 infections and ~10% fatality rate in humans (14, 15). Middle
79 East respiratory syndrome coronavirus (MERS-CoV) was identified in 2012 and has so
80 far caused over 2200 infections and ~35% fatality rate in humans (16, 17). An envelope-
81 anchored spike protein guides coronavirus entry into host cells (18, 19). It first binds to a
82 receptor on host cell surface for viral attachment through its S1 subunit, and then fuses

83 viral and host membranes through its S2 subunit. The membrane fusion step by
84 coronavirus spikes requires two prior cleavages by host proteases: the first at the S1/S2
85 boundary (i.e., S1/S2 site) and the second within S2 (i.e., S2' site) (8, 19-21). Depending
86 on the virus, the spike-processing proteases may come from different stages of the
87 coronavirus infection cycle. For MERS-CoV, its spike can be processed by proprotein
88 convertases (e.g., furin) during the molecular maturation process in virus-producing cells,
89 by cell-surface proteases (e.g., transmembrane protease serine 2 or TMPRSS2) after viral
90 attachment, and by lysosomal proteases (e.g., cathepsins) after endocytosis in virus-
91 targeted cells (22-26). It was previously reported that MERS-CoV spike could be
92 processed by furin after viral endocytosis in virus-targeted cells (21), but this finding was
93 not supported by a recent study (27). The protease activation pattern of SARS-CoV entry
94 is similar to that of MERS-CoV, except that SARS-CoV spike can also be processed by
95 extracellular proteases (e.g., elastase) after viral release (20, 28-30). It has been suggested
96 that the tissue tropisms of MERS-CoV and SARS-CoV are correlated with the tissue
97 distributions of proprotein convertases, extracellular proteases, and cell-surface proteases
98 in the host (22, 23, 26, 29-31). For example, the availability of trypsin-like proteases in
99 the respiratory tracts has been suggested to be a determinant of the respiratory tropism of
100 SARS-CoV (29, 30). However, although coronavirus entry also depends on lysosomal
101 proteases, it is not clear whether the species and tissue tropism of coronaviruses are
102 correlated with differential lysosomal protease activities from different hosts or tissue
103 cells.

104 Both MERS-CoV and SARS-CoV are thought to have originated from bats.
105 SARS-like coronaviruses isolated from bats and SARS-CoV isolated from humans are

106 genetically highly similar to each other; some of the bat SARS-like coronaviruses
107 recognize the same receptor angiotensin-converting enzyme 2 (ACE2) as human SARS-
108 CoV (32-35). MERS-like coronaviruses isolated from bats and MERS-CoV isolated from
109 humans so far are also genetically similar to each other, albeit not as similar as between
110 bat SARS-like coronaviruses and human SARS-CoV (36-39). Several MERS-like
111 coronaviruses from bats, including HKU4, recognize the same receptor dipeptidyl
112 peptidase 4 (DPP4) as MERS-CoV (24, 40-43). Moreover, human lysosomal proteases
113 only activate the MERS-CoV spike, but not the HKU4 spike, for viral entry into human
114 cells, while bat lysosomal proteases activate both MERS-CoV and HKU4 spikes for viral
115 entry into bat cells (44). Furthermore, the expression level of lysosomal proteases in
116 human lung cells is lower than in human liver cells, leading to inefficient activation of
117 MERS-CoV spike by lysosomal proteases in human lung cells (45). These results point to
118 the possibility that lysosomal protease activities differ among cells from different hosts or
119 even among cells from the same host species, restricting coronavirus entry and their
120 tropism. However, these studies did not control the contribution from host receptors,
121 despite the fact that receptor homologues from different host species may differ in their
122 functions as coronavirus receptors or that the same receptor protein may be expressed at
123 different levels in different tissues within one host species. Moreover, these studies were
124 carried out at the cellular level, and did not provide direct biochemical evidence to
125 demonstrate that lysosomal proteases from human and bat cells process coronavirus
126 spikes differentially. Therefore, factor-controlled viral entry data and direct biochemical
127 data are both needed to critically and directly establish the correlation between lysosomal
128 protease activities and coronavirus tropism.

129 In this study, we controlled the contributions from receptor binding and other
130 proteases, and our data support the hypothesis that differential lysosomal protease
131 activities from bat and human cells impact the efficiency of coronavirus entry into these
132 cells. We also purified lysosomal extracts from bat and human cells and showed that bat
133 and human lysosomal proteases differentially process coronavirus spikes and activate
134 coronavirus entry. Overall, this study provides the first direct evidence supporting the
135 notion that differential lysosomal protease activities are an important determinant of the
136 species and tissue tropism of coronaviruses.

137

138 **Results**

139 *Screening for cells that are suitable for studying lysosomal-proteases-activated*
140 *coronavirus entry*

141 To study lysosomal-proteases-activated coronavirus entry, we must carefully
142 control for the contributions from the host receptor and other intracellular and
143 extracellular proteases, such that coronavirus-spike-mediated viral entry would be solely
144 or mainly dependent on the contribution from lysosomal proteases. In other words, we
145 partition the membrane fusion process from the receptor binding step and also separate
146 the effects of lysosomal proteases from the other proteases that may participate in
147 coronavirus entry. To this end, we screened for cell lines that met the following three
148 criteria: (i) The cells from different species or tissues endogenously must express no or
149 low levels of receptor protein for the coronavirus of interest, such that they can be
150 controlled to exogenously express the receptor protein from a single host species; (ii) The
151 cells must express no or low level of cell-surface proteases, such that lysosomal proteases

152 from these cells are the only or main cellular proteases that activate the membrane fusion
153 process for the coronavirus of interest (proprotein convertases are not a factor here
154 because the same batch of viruses, which had gone through the same molecular
155 maturation process, would be used to infect different cells); (iii) The cells can be
156 transfected easily, such that the cells from different origins can be controlled to express
157 similar levels of the receptor protein from a single host species. In sum, we were looking
158 for cells that are both “naked” (not expressing or expressing low levels of coronavirus
159 receptor or cell-surface proteases) and “easily transfectable”.

160 To identify and exclude those cells that endogenously express coronavirus
161 receptors, we performed coronavirus-spike-mediated pseudovirus entry in a number of
162 human, monkey and bat cell lines. To this end, retroviruses pseudotyped with the MERS-
163 CoV or SARS-CoV spike (i.e., MERS-CoV pseudoviruses or SARS-CoV pseudoviruses,
164 respectively) were used to test the endogenous levels of receptor expression from
165 different cell lines including human kidney cells (HEK293T), human cervix cells (HeLa),
166 human liver cells (Huh7), human lung cells (A549 and MRC5), monkey kidney cells
167 (Vero), bat kidney cells (RSKT and BKD9), and bat lung cells (PESU-B5L and Tb1-Lu).
168 The results showed that among these cells, Huh7 cells, Vero cells, MRC5 cells, PESU-
169 B5L cells, and RSKT cells all supported significant levels of MERS-CoV pseudovirus
170 entry, suggesting that these cells endogenously express significant levels of DPP4 (either
171 human, monkey, or bat DPP4, depending on the cell origin) (Fig. 1A). In contrast, only
172 Vero cells and RSKT cells supported significant levels of SARS-CoV pseudovirus entry,
173 suggesting that these cells endogenously express significant levels of ACE2 (monkey and
174 bat ACE2, respectively) (Fig. 1B). These results are largely consistent with previous

175 studies with two exceptions: previous studies showed that PESU-B5L cells do not
176 support the infection of MERS-CoV and that Huh7 cells support the infection of SARS-
177 CoV (35, 40, 44, 46-48). Overall, the cells that endogenously express significant levels of
178 DPP4 or ACE2 were not suitable for studying the roles of lysosomal proteases in
179 coronavirus entry and hence were excluded from downstream studies.

180 To investigate which of the cells can be controlled to exogenously express
181 significant levels of coronavirus receptors, we transfected these cells with a plasmid
182 encoding human DPP4. We then performed Western blotting using an antibody
183 recognizing the C-terminal C9 tag of exogenously expressed human DPP4 in these cells
184 (Fig. 1C). The result showed that: (i) HEK293T cells, HeLa cells, and Tb1-Lu cells
185 exogenously express significant levels of human DPP4; (ii) Huh7 cells, A549 cells, Vero
186 cells, and MRC5 cells exogenously express low levels of human DPP4; (iii) PESU-B5L
187 cells, RSKT cells, and BKD9 cells do not exogenously express human DPP4. Therefore,
188 HEK293T, HeLa cells, and Tb1-Lu cells were selected for downstream studies designed
189 to evaluate the roles of lysosomal proteases in coronavirus entry because they met two of
190 the three aforementioned criteria: they are naked without endogenously expressing
191 coronavirus receptors, and they are easily transfectable and hence can be controlled to
192 exogenously express coronavirus receptors. In addition, an MTT cell viability assay
193 showed that the viabilities of these three types of cells were not affected by the presence
194 of different protease inhibitors, allowing the use of these protease inhibitors in
195 characterizing the roles of different proteases in coronavirus entry (Fig. 1D).
196 Furthermore, as shown below, they are also naked with no or low endogenous expression

197 of cell-surface proteases. Characterization and selection of these cells laid the foundation
198 for defining the roles of lysosomal proteases in coronavirus entry.

199 *Lysosomal proteases from human and bat cells activate coronavirus-spike-mediated*
200 *membrane fusion differentially*

201 To examine the role of lysosomal proteases in MERS-CoV-spike-mediated
202 membrane fusion, we performed MERS-CoV pseudovirus entry in the three model cell
203 lines where exogenous expression of human DPP4 can be measured and calibrated:
204 human HEK293T cells (h-HEK293T), human HeLa cells (h-HeLa), and bat Tb1-Lu cells
205 (b-Tb1-Lu). The results showed that all three types of cells supported MERS-CoV
206 pseudovirus entry at significant levels when they exogenously expressed human DPP4
207 (Fig. 2A). After the expression levels of cell surface-associated human DPP4 were
208 measured and calibrated across the three types of cells (Fig. 2A), b-Tb1-Lu cells
209 supported MERS-CoV pseudovirus entry more efficiently than both h-HeLa cells and b-
210 Tb1-Lu cells. Because no extracellular protease was added to the pseudovirus entry
211 assay, there data suggest that cellular proteases were responsible for the highest
212 efficiency of b-Tb1-Lu cells in activating MERS-CoV pseudovirus entry. MERS-CoV
213 pseudovirus entry in the presence of different cellular protease inhibitors showed that
214 lysosomal protease (i.e., cathepsins) inhibitor almost completely inhibited MERS-CoV
215 pseudovirus entry into these cells, whereas proprotein convertase (i.e., furin) inhibitor
216 and cell-surface protease (i.e., TMPRSS2) inhibitor had much less impact on the
217 efficiency of these cells in supporting MERS-CoV pseudovirus entry (Fig. 2A). Thus,
218 lysosomal proteases were mainly responsible for MERS-CoV pseudovirus entry into

219 these cells. Therefore, after the contributions from host receptor and other proteases were
220 controlled, lysosomal proteases from b-Tb1-Lu cells supported MERS-CoV-spike-
221 mediated membrane fusion more efficiently than their counterparts from h-HEK293T
222 cells and h-HeLa cells.

223 To further demonstrate that differential lysosomal protease activities directly
224 impact MERS-CoV-spike-mediated membrane fusion, we performed MERS-CoV-spike-
225 mediated cell-cell fusion in the presence of purified lysosomal extracts from different
226 cells. To this end, we purified lysosomal extracts from h-HEK293T cells, h-HeLa cells,
227 b-Tb1-Lu cells, and bat BKD9 (b-BKD9) cells. Subsequently, we mixed one batch of h-
228 HEK293T cells exogenously expressing the MERS-CoV spike and another batch of h-
229 HEK293T cells exogenously expressing human DPP4. Then we added the same amount
230 (in mass) of each of the lysosomal extracts to the mixture of the above h-HEK293T cells,
231 while reducing the pH of the cell culture medium to where lysosomal proteases were
232 active (i.e., pH 5.6). As we showed earlier, h-HEK293T cells do not endogenously
233 express significant amount of cell-surface proteases (Fig. 2A). Hence, the efficiency of
234 cell-cell fusion likely reflects the activation of MERS-CoV-spike-mediated membrane
235 fusion by purified lysosomal extracts from different types of cells. The result showed that
236 lysosomal extracts from b-Tb1-Lu cells and b-BKD9 cells both activate MERS-CoV-
237 spike-mediated cell-cell fusion more efficiently than their counterparts from h-HEK293T
238 cells and h-HeLa cells (Fig. 2B). In comparison, in the absence of any lysosomal extracts,
239 there was no significant cell-cell fusion at neutral pH and only low level of cell-cell
240 fusion at low pH, suggesting that pH alone has no or little effect on MERS-CoV-spike-
241 mediated cell-cell fusion (Fig. 2B). Therefore, consistent with MERS-CoV pseudovirus

242 entry assay, cell-cell fusion assay also revealed that lysosomal extracts from bat cells
243 support MERS-CoV-spike-mediated membrane fusion more efficiently than their
244 counterparts from human cells.

245 To examine the purity of these lysosomal extracts, we investigated potential
246 contaminations of the lysosomal extracts by proteins from plasma or endoplasmic
247 reticulum (ER). Because alkaline phosphatase (ALP) and cytochrome P450 reductase
248 (CPR) are markers of plasma enzymes and ER enzymes, respectively, their activities in
249 lysosomal extracts are commonly used as indicators of the purities of lysosomal extracts
250 (49). Hence we measured the ALP and CPR activities of the lysosomal extracts from
251 different cell lines (Fig. 3A, 3B). The results showed that compared to the whole cell
252 lysates, the ALP and CPR activities in the lysosomal extracts were low (for some
253 unknown reason, the ALP activities of BKD9 cells were very low). Thus based on these
254 indicator proteins, the contaminations of the lysosomal extracts by plasma and ER
255 proteins are low.

256 To extend the above findings from MERS-CoV to other coronaviruses, we
257 investigated whether lysosomal proteases from human and bat cells activate SARS-CoV-
258 spike-mediated membrane fusion differentially, also after controlling the contributions
259 from host receptor and other proteases. To this end, we performed SARS-CoV
260 pseudovirus entry into h-HEK293T cells, h-HeLa cells, and b-Tb1-Lu cells, all of which
261 were controlled to exogenously express human ACE2. The result showed that like
262 MERS-CoV pseudoviruses, SARS-CoV pseudoviruses entered b-Tb1-Lu cells more
263 efficiently than they did h-HEK293T and h-HeLa cells (Fig. 4A). Lysosomal protease

264 inhibitor almost completely inhibited SARS-CoV pseudovirus entry into these cells,
265 while proprotein convertase inhibitor and cell-surface protease inhibitor had much less
266 impact on SARS-CoV pseudovirus entry into these cells. Hence, lysosomal proteases
267 were the main contributor to SARS-CoV pseudovirus entry into these cells. Moreover,
268 we carried out SARS-CoV-spike-mediated cell-cell fusion in the presence of lysosomal
269 extracts from h-HEK293T cells, h-HeLa cells, b-Tb1-Lu cells, or b-BKD9 cells. The
270 result showed that lysosomal extracts from bat cells activated SARS-CoV-spike-mediated
271 cell-cell fusion more efficiently than their counterparts from human cells (Fig. 4B).
272 Taken together, our data support the hypothesis that lysosomal proteases from bat cells
273 support SARS-CoV-spike-mediated membrane fusion, in the forms of both pseudovirus
274 entry and cell-cell fusion, more efficiently than their counterparts from human cells.

275 *Lysosomal proteases from human and bat cells process MERS-CoV spike differentially*

276 To provide direct biochemical evidence supporting that lysosomal proteases from
277 human and bat cells process MERS-CoV spike differentially, we digested cell-surface-
278 expressed MERS-CoV spike using lysosomal extracts from human and bat cells. To this
279 end, we exogenously expressed MERS-CoV spike on the surface of h-HEK293T cells. In
280 the meanwhile, we purified lysosomal extracts from different types of human and bat
281 cells. Then we incubated the cell-surface-expressed MERS-CoV spike with the same
282 amount of lysosomal extracts from each type of the cells, and we performed Western
283 blotting analysis to detect the cleavage state of MERS-CoV spike. The result showed that
284 more than half of the MERS-CoV spike molecules had been cleaved to S2 by proprotein
285 convertases during the molecular maturation process, and that lysosomal extracts from

286 bat cells were more efficient than their counterparts from human cells in further cleaving
287 MERS-CoV spike to produce S2' fragments (Fig. 5A). Between the two types of bat
288 cells, lysosomal extracts from b-BKD9 cells processed MERS-CoV spike more
289 efficiently than their counterparts from b-Tb1-Lu cells. We further compared the
290 lysosomal extracts from b-BKD9 cells and their counterparts from h-HEK293T cells:
291 lysosomal extracts from b-BKD9 cells processed MERS-CoV spike much more
292 efficiently than their counterparts from h-HEK293T cells in a time-dependent manner
293 (Fig. 5B). Overall, lysosomal extracts from bat cells demonstrated higher efficiency in
294 processing MERS-CoV spike than their counterparts from human cells.

295 To further compare the coronavirus-spike-processing activities of human and bat
296 lysosomal proteases, we examined whether lysosomal extracts from human and bat cells
297 process the spike protein from a MERS-like bat coronavirus HKU4 differentially.
298 Previously we showed that HKU4 spike contains a glycosylated lysosomal protease site
299 at the S1/S2 boundary and it mediates virus entry into bat cells, but not human cells (44).
300 Here we investigated direct biochemical evidence for the differential HKU4-spike-
301 processing activities of human and bat lysosomal proteases. To this end, we purified
302 lysosomal extracts from h-HEK293T cells and b-Tb1-Lu cells, and incubated them
303 individually with HKU4 spike expressed on the surface of h-HEK293T cells. The result
304 showed that lysosomal extracts from b-Tb1-Lu cells, but not their counterparts from h-
305 HEK293T cells, cleaved HKU4 spike containing a glycosylated lysosomal protease motif
306 to produce S2 (Fig. 6A). Next we introduced an N762A mutation into HKU4 spike; the
307 mutation had been shown to remove the glycosylation from the lysosomal protease motif
308 in HKU4 spike (44). The result showed that lysosomal extracts from both h-HEK293T

309 cells and b-Tb1-Lu cells cleaved the mutant HKU4 spike to produce S2 (Fig. 6B). These
310 results provided direct biochemical evidence demonstrating that lysosomal extracts from
311 b-Tb1-Lu cells, but not their counterparts from h-HEK293T cells, can process the
312 glycosylated lysosomal protease motif in HKU4 spike, whereas lysosomal extracts from
313 both h-HEK293T cells and b-Tb1-Lu cells can process the unglycosylated lysosomal
314 protease motif in HKU4 spike.

315 **Discussion**

316 The tropism of coronaviruses includes their species and tissue tropism (1).
317 Lysosomal proteases play a critical role in coronavirus entry (8, 10, 11), but their roles in
318 coronavirus tropism have not been critically established. In contrast, extracellular
319 proteases and other cellular proteases have been shown to be important determinants of
320 coronavirus tropism (22, 23, 26, 29-31). We and others previously showed that a MERS-
321 like coronavirus from bats, HKU4, uses the same host receptor DPP4 as MERS-CoV (24,
322 41), and we also showed that cellular proteases from bat and human cells differentially
323 support HKU4 entry (24, 44). However, two factors can complicate the roles of
324 lysosomal proteases in coronavirus tropism: human and bat DPP4 molecules have
325 different activities as coronavirus receptors, and other proteases may also play significant
326 roles in the cell entry process of coronaviruses. In the current study, we quantified and
327 controlled the contributions from host receptor and other proteases to coronavirus entry,
328 such that the role of lysosomal proteases could be clearly defined in coronavirus entry
329 into cells from different origins. To this end, we screened a number of cell lines
330 originated from different tissues and host species and found three types of cells that were

331 suitable for studying the roles of lysosomal proteases in coronavirus tropism: human
332 HEK293T cells, human HeLa cells, and bat Tb1-Lu cells. These three types of cells share
333 the following common features: they are “naked” for endogenously expressing very low
334 levels of coronavirus receptor or cell-surface proteases, and they can be easily transfected
335 to exogenously express the coronavirus receptor from a single host species. As a result,
336 lysosomal proteases likely function as the only or main contributor to coronavirus-spike-
337 mediated entry. The above approach and findings may be extended to study the roles of
338 lysosomal proteases in the entry of other viruses.

339 The current study investigated the roles of lysosomal proteases from the above
340 human and bat cells in coronavirus entry using a combination of pseudovirus entry, cell-
341 cell fusion, and biochemical assays. To this end, we exogenously expressed human DPP4
342 in different types of cells, and performed MERS-CoV-spike-mediated pseudovirus entry
343 and cell-cell fusion. In the presence of DPP4 from the same species and in the absence of
344 extracellular proteases and other cellular proteases, lysosomal proteases and lysosomal
345 extracts from bat cells supported MERS-CoV-spike-mediated membrane fusion more
346 efficiently than their counterparts from human cells. These observations were then
347 extended to SARS-CoV-spike-mediated pseudovirus entry and cell-cell fusion.
348 Moreover, we prepared lysosomal extracts from human and bat cells, and showed that
349 lysosomal extracts from bat cells cleaved MERS-CoV spike more efficiently than their
350 counterparts from human cells. We also showed that lysosomal extracts from bat cells
351 cleaved HKU4 spike, which contains a glycosylated lysosomal protease motif, more
352 efficiently than their counterparts from human cells. These results demonstrated that the
353 spike proteins from MERS-CoV, SARS-CoV, and HKU4 all mediated viral entry into bat

354 cells at higher efficiency than into human cells, due to or mainly due to the higher
355 coronavirus-spike-processing activities of bat lysosomal proteases.

356 The correlation between lysosomal protease activities and coronavirus tropism is
357 a novel finding in virology. Previous studies already showed that the expression levels of
358 lysosomal proteases vary among different tissues within the same host species, due to the
359 different physiological functions of tissue cells (7, 45). Our study demonstrates that
360 lysosomal protease activities may also vary among different mammalian species,
361 indicating that adaptation of coronaviruses to new species may occur through adaptation
362 to different lysosomal protease activities. The physiological reason behind different
363 lysosomal protease activities among mammalian species is not clear, but it could be due
364 to different lifestyles of these species. For instance, although speculative, bats are the
365 only flying mammals and hence the enhanced lysosomal protease activities of bat cells
366 may provide fast turnover of metabolic products and also produce high levels of
367 nutrients. In this sense, supporting coronavirus entry efficiently could be a byproduct of
368 the enhanced lysosomal protease activities of bat cells. It is worth noting that due to the
369 difficulty in culturing bat tissue cells, this study was performed using bat cell lines.
370 Although cell lines usually maintain many features of original tissue cells, these findings
371 will need to be confirmed using bat tissue cells. Our study suggests that no matter
372 whether cells are from different host species or from different tissues of the same host
373 species, those cells with higher lysosomal protease activities in general support
374 coronavirus entry more efficiently than the cells with lower lysosomal proteases do. It
375 remains to be further investigated whether the higher lysosomal protease activities in
376 some cells are due to enhanced enzymatic activities, elevated expression levels, or some

377 other changes that happened to their lysosomal proteases. Nevertheless, our study has
378 established that differential lysosomal proteases from different types of cells have direct
379 impact on coronavirus entry, which has implications for the tissue and species tropism of
380 coronaviruses.

381

382 **Acknowledgements**

383 This work was supported by NIH grants R01AI089728 (to F.L.) and
384 R01AI110700 (to F.L. and R.B.).

385

386

387

388

389 **Materials and Methods**

390 *Cell lines and plasmids*

391 HEK293T cells (human embryonic kidney cells), HeLa cells (human cervical
392 epithelial cells), A549 cells (human alveolar epithelial cells), Vero cells (monkey kidney
393 cells), MRC5 cells (human lung cells), Tb1-Lu cells (*Triatoma brasiliensis* bat lung cells)
394 were obtained from ATCC (the American Type Culture Collection). RSKT cells
395 (*Rhinolophus sinicus* bat kidney cells), PESU-B5L cells (*Perimyotis subflavus* bat lung
396 cells), and BKD9 cells (*Myotis davidii* bat kidney cells) were purchased from Sigma-
397 Aldrich. Huh-7 cells (human hepatoma cells) were kindly provided by Dr. Charles M.
398 Rice at Rockefeller University. All cells were cultured in DMEM supplemented with
399 10% FBS, 2 mM L-glutamine, 100 units/ml penicillin, and 100 µg/ml streptomycin (Life
400 Technologies). The full-length genes of MERS-CoV spike (GenBank accession number
401 AFS88936.1), SARS-CoV spike (GenBank accession number AFR58742), human DDP4
402 (GenBank accession number NM_001935.3) and human ACE2 (GenBank accession
403 number NM_021804) were synthesized (Genscript Biotech.) and subcloned into the
404 pcDNA3.1(+) vector (Life Technologies) with a C-terminal C9 tag. Plasmids (pFR-Luc
405 and pBD-NFκB) for cell-cell fusion are kindly provided by Dr. Zhaohui Qian at the
406 Chinese Academy of Medical Sciences and Peking Union Medical College.

407 *Coronavirus-spike-mediated pseudovirus entry into human and bat cells*

408 Retroviruses pseudotyped with MERS-CoV or SARS-CoV spike protein (i.e.,
409 MERS-CoV pseudoviruses or SARS-CoV pseudoviruses, respectively) were generated as
410 described previously (24). Briefly, HEK293T cells were co-transfected with a plasmid
411 carrying an Env-defective, luciferase-expressing HIV-1 genome (pNL4-3.luc.R-E-) and

412 pcDNA3.1(+) plasmid encoding MERS-CoV or SARS-CoV spike. Pseudoviruses were
413 harvested 72 hours after transfection, and were used to enter human and bat cells. For
414 screening of cell lines expressing no or low levels of coronavirus receptor, different types
415 of cells were seeded in 96-well plates and infected immediately by pseudoviruses. For
416 studying the roles of lysosomal proteases in coronavirus entry, cells were transfected with
417 pcDNA3.1(+) plasmid encoding human DPP4 or human ACE2. 24 hours after the
418 transfection, the cells expressing the receptor were seeded in 96-well plates and then
419 infected by pseudoviruses. After incubation at 37 °C for 6 hours, the medium was
420 replaced with fresh DMEM. After another 60 hours, cells were washed with PBS and
421 lysed. Aliquots of cell lysates were transferred to an Optiplate-96 plate (PerkinElmer Life
422 Sciences), and then luciferase substrate (Promega) was added. Relative luciferase units
423 were measured using EnSpire plate reader (PerkinElmer Life Sciences), and normalized
424 for exogenous expression levels of the corresponding receptor in cell membranes (see
425 below).

426 Inhibition of pseudovirus entry using various protease inhibitors was carried out
427 as described previously (50). Briefly, target cells were preincubated with medium
428 containing a final concentration of 50 μ M camostat mesylate (Sigma-Aldrich), 50 μ M E-
429 64d (Sigma-Aldrich), 50 μ M Chloromethylketone (Enzo), or DMSO (negative control) at
430 37 °C for 1 hour. The cells were subsequently infected by pseudoviruses. The cells were
431 incubated at 37 °C for 6 to 8 hours, and then the medium was replaced with fresh
432 DMEM. After another 48 hours, the cells were lysed and measured for luciferase activity.

433 *Exogenous expression of coronavirus receptor in cells and cell surfaces*

434 To examine the exogenous expression level of coronavirus receptor in whole cell
435 lysates, cells were transfected with pcDNA3.1(+) plasmid encoding human DPP4 or
436 human ACE2 containing a C-terminal C9 tag. 48 hours after transfection, the cells were
437 lysed using ultrasonication, and aliquots of cell lysates were subjected to Western
438 blotting analysis. The C9-tagged coronavirus receptors were detected using an anti-C9
439 tag monoclonal antibody (Santa Cruz Biotechnology). The current assay measures the
440 total expression level of coronavirus receptor in a certain amount of cells, without
441 specifying how many of these cells were transfected or how much protein was expressed
442 in each transfected cell.

443 To examine the exogenous expression level of coronavirus receptor in cell
444 membranes, the cells expressing the receptor were harvested as above and all membrane-
445 associated proteins were extracted using the Membrane Protein Extraction Kit (Thermo
446 Fisher Scientific). Briefly, cells were centrifuged at $300 \times g$ for 5 minutes and washed
447 with Cell Wash Solution twice. The cell pellets were resuspended in 0.75 mL
448 Permeabilization Buffer and incubated at 4°C for 10 minutes. The supernatant containing
449 cytosolic proteins was removed after centrifugation at $16,000 \times g$ for 15 minutes. The
450 pellets containing membrane-associated proteins were resuspended in 0.5 mL
451 Solubilization Buffer and incubated at 4°C for 30 minutes. After centrifugation at $16,000$
452 $\times g$ for 15 minutes, the membrane-associated proteins from the supernatant were
453 transferred to a new tube. The expression level of membrane-associated C9-tagged
454 coronavirus receptor among the membrane-associated proteins was then measured using
455 Western blot analysis as above, and further used for normalizing the results from
456 pseudovirus entry assays. Although the current assay could not differentiate between

457 plasma membrane-associated proteins and internal membrane-associated proteins, ACE2
458 and DPP4 are known to be strongly associated with plasma membranes due to their
459 respective plasma-membrane-targeting signal peptide (51, 52).

460 *MTT assay*

461 Cells were seeded in 96-well plates and treated with DMSO or DMSO-dissolved
462 protease inhibitors at 37 °C. After incubation for 6 hours, the medium was replaced with
463 fresh DMEM. After incubation for 70 hours at 37 °C, 10 µL MTT solution (Biotium) was
464 added to each well and mixed with the medium. After incubation at 37 °C for 2 hours,
465 200 µL DMSO or DMSO-dissolved protein inhibitor was added to each well and mixed
466 with the medium. The MTT signal was measured as absorbance at 570 nm using Synergy
467 2 multi-mode microplate reader (BioTek Instruments).

468 *Preparation of lysosomal extracts*

469 Lysosomal extracts from human or bat cells were prepared according to the
470 lysosome isolation kit procedure (Sigma-Aldrich). Briefly, cells were harvested and
471 washed by PBS buffer, and then resuspended by 2.7 PCV (i.e., packed cell volume)
472 extraction buffer. Cells were broken in a 7 ml Dounce homogenizer using a loose pestle
473 (i.e., Pestle B) until 80%-85% of cells were broken (protease inhibitors from the kit were
474 omitted in our procedure). The samples were centrifuged at 1,000xg for 10 min, and the
475 supernatants were transferred to a new centrifuge tube and centrifuged at 20,000xg for
476 another 20 min. The supernatants were removed, and then the pellets were resuspended in
477 extraction buffer as CLF (crude lysosomal fraction). The CLF was diluted in buffer
478 containing 19% Optiprep Density Gradient Medium Solution and further purified using
479 density gradient centrifugation at 150,000xg for 4 hours to yield lysosomal extracts. The

480 concentrations of the lysosomal extracts were measured using a NanoDrop 8000 (Thermo
481 Fisher Scientific) and calculated according to their absorbance at 280 nm. The purities of
482 the lysosomal extracts were examined using the following assays.

483 Cytochrome P450 reductase (CPR) is an endoplasmic reticulum (ER) marker. For
484 evaluation of the potential contamination of the purified lysosomal extracts by ER
485 proteins, cytochrome P450 reductase activity of the purified lysosomal extracts was
486 measured using the cytochrome P450 reductase assay kit (Biovision). Briefly, a glucose-
487 6-phosphate (G6P) standard curve was first calculated through mixing a series of
488 volumes of 1 mM G6P standard solution with 5 μ l NADPH substrate and 5 μ l G6P
489 Standard Developer to make the final volume 100 μ l/well. The well contents were then
490 mixed and incubated at room temperature for at least 30 min (protected from light).
491 Absorbance at 460 nm was measured. Then 5 μ l lysosomal extracts from different cell
492 lines were mixed with 55 μ l CPR assay buffer. After adding 30 μ l of the assay reaction
493 mixture to each well and incubating the solutions at room temperature for 5 min, 10 μ l of
494 the 20 mM G6P solution was added to each well. Absorbance at 460 nm was measured
495 immediately in kinetic mode at 25 °C for 25 min using Synergy 2 multi-mode microplate
496 reader (BioTek Instruments). Calculation of the cytochrome P450 reductase activity was
497 performed according to the manufacturer's manual.

498 Alkaline phosphatase (ALP) is a plasma enzyme marker. For evaluation of the
499 potential contamination of the purified lysosomal extracts by plasma proteins, alkaline
500 phosphatase activity of the purified lysosomal extracts was measured using alkaline
501 phosphatase assay kit (Abnova). Briefly, a standard curve was first calculated through
502 mixing a series of concentrations of 4-Methylumbelliferyl phosphate disodium salt

503 (MUP) standard with 10 μ l ALP enzyme solution. The reactions were incubated at 25 °C
504 for 30 min (protected from light). The ALP enzyme can convert MUP substrate to equal
505 molar amount of fluorescent 4-Methylumbelliferone (4-MU). Hence 20 μ l 0.5 mM MUP
506 substrate solution was added to each well containing 5 μ l lysosomal extracts from
507 different cell lines. After mixing and incubating at 25 °C for 30 min (protected from
508 light), all reactions were stopped through adding 20 μ L stop solution into each reaction.
509 Then fluorescence intensities at Ex/Em 360/440 nm were measured using Synergy 2
510 multi-mode microplate reader (BioTek Instruments). Calculation of the alkaline
511 phosphatase activity was performed according to the manufacturer's manual.

512 *Coronavirus-spike-mediated cell-cell fusion*

513 Cell-cell fusion was performed as described previously (53). Briefly, to produce
514 cells expressing one of the coronavirus spikes, HEK293T cells were co-transfected with
515 plasmid pFR-Luc, which contains a synthetic promoter with five tandem repeats of the
516 yeast GAL4 binding sites that controls expression of the luciferase gene, and
517 pcDNA3.1(+) plasmid encoding one of the coronavirus spikes. To produce cells
518 expressing one of the corresponding coronavirus receptor proteins, HEK293T cells were
519 co-transfected with pBD-NF-kappaB, which encodes a fusion protein with the DNA
520 binding domain of GAL4 and transcription activation domain of NF-kappaB, and
521 pcDNA3.1(+) plasmid encoding one of the corresponding coronavirus receptor proteins.
522 After culturing for 24 hours, the spike-expressing HEK293T cells were lifted,
523 centrifuged, and then resuspended in low pH medium containing 10 mM sodium citrate
524 pH 5.6. Subsequently the spike-expressing HEK293T cells were treated with purified
525 lysosomal extracts (100 μ g/ml) in the low pH medium. After incubation at 37 °C for 30

526 minutes, spike-expressing cells were centrifuged, resuspended in fresh neutral pH
527 medium, and then overlaid onto receptor-expressing HEK293T cells at a ratio of 1:2.
528 When cell-cell fusion occurred, the expression of the luciferase gene would be activated
529 through binding of the GAL4-NF-kappaB fusion protein to GAL4 binding sites at the
530 promoter of the luciferase gene. After incubation for 24 hours, the cells were lysed, the
531 aliquots of cell lysates were transferred to an Optiplate-96 plate (PerkinElmer Life
532 Sciences), and then luciferase substrate (Promega) was added. Relative luciferase units
533 were measured using EnSpire plate reader (PerkinElmer Life Sciences).

534 *Cleavage of coronavirus spikes using purified lysosomal extracts*

535 HEK293T cells were transfected with pcDNA3.1(+) plasmid encoding MERS-
536 CoV spike or HKU4 spike. 48 hours after transfection, the cells were harvested and
537 washed by PBS buffer. The cells were then treated with 50 µg/ml purified lysosomal
538 extracts at pH 5.6 for 30 minutes or 100 µg/ml purified lysosomal extracts at pH 5.6 for
539 different periods of time (i.e., 10, 30, 60 minutes). After treatment, the cells were lysed
540 and boiled for Western blotting analysis. The C9-tagged spikes were detected using an
541 anti-C9 tag monoclonal antibody (Santa Cruz Biotechnology).
542

543 **References**

- 544 1. **Nomaguchi M, Fujita M, Miyazaki Y, Adachi A.** 2012. Viral tropism. *Front*
545 *Microbiol* **3**:281.
- 546 2. **Dimitrov DS.** 2004. Virus entry: molecular mechanisms and biomedical
547 applications. *Nat Rev Microbiol* **2**:109-122.
- 548 3. **Skehel JJ, Wiley DC.** 2000. Receptor binding and membrane fusion in virus
549 entry: The influenza hemagglutinin. *Annual Review of Biochemistry* **69**:531-569.
- 550 4. **Li WH, Wong SK, Li F, Kuhn JH, Huang IC, Choe H, Farzan M.** 2006.
551 Animal origins of the severe acute respiratory syndrome coronavirus: Insight from
552 ACE2-S-protein interactions. *Journal of Virology* **80**:4211-4219.
- 553 5. **Luzio JP, Pryor PR, Bright NA.** 2007. Lysosomes: fusion and function. *Nat Rev*
554 *Mol Cell Biol* **8**:622-632.
- 555 6. **Lim CY, Zoncu R.** 2016. The lysosome as a command-and-control center for
556 cellular metabolism. *J Cell Biol* **214**:653-664.
- 557 7. **Turk V, Stoka V, Vasiljeva O, Renko M, Sun T, Turk B, Turk D.** 2012.
558 Cysteine cathepsins: from structure, function and regulation to new frontiers.
559 *Biochim Biophys Acta* **1824**:68-88.
- 560 8. **Millet JK, Whittaker GR.** 2015. Host cell proteases: Critical determinants of
561 coronavirus tropism and pathogenesis. *Virus Res* **202**:120-134.
- 562 9. **Hunt CL, Lennemann NJ, Maury W.** 2012. Filovirus entry: a novelty in the
563 viral fusion world. *Viruses* **4**:258-275.
- 564 10. **Simmons G, Gosalia DN, Rennekamp AJ, Reeves JD, Diamond SL, Bates P.**
565 2005. Inhibitors of cathepsin L prevent severe acute respiratory syndrome
566 coronavirus entry. *Proceedings of the National Academy of Sciences of the*
567 *United States of America* **102**:11876-11881.

- 568 11. **Simmons G, Reeves JD, Rennekamp AJ, Amberg SM, Piefer AJ, Bates P.**
569 2004. Characterization of severe acute respiratory syndrome-associated
570 coronavirus (SARS-CoV) spike glycoprotein-mediated viral entry. Proceedings of
571 the National Academy of Sciences of the United States of America **101**:4240-
572 4245.
- 573 12. **Enjuanes L, Almazan F, Sola I, Zuniga S.** 2006. Biochemical aspects of
574 coronavirus replication and virus-host interaction. *Annu Rev Microbiol* **60**:211-
575 230.
- 576 13. **Perlman S, Netland J.** 2009. Coronaviruses post-SARS: update on replication
577 and pathogenesis. *Nature Reviews Microbiology* **7**:439-450.
- 578 14. **Ksiazek TG, Erdman D, Goldsmith CS, Zaki SR, Peret T, Emery S, Tong**
579 **SX, Urbani C, Comer JA, Lim W, Rollin PE, Dowell SF, Ling AE,**
580 **Humphrey CD, Shieh WJ, Guarner J, Paddock CD, Rota P, Fields B, DeRisi**
581 **J, Yang JY, Cox N, Hughes JM, LeDuc JW, Bellini WJ, Anderson LJ.** 2003.
582 A novel coronavirus associated with severe acute respiratory syndrome. *New*
583 *England Journal of Medicine* **348**:1953-1966.
- 584 15. **Peiris JSM, Lai ST, Poon LLM, Guan Y, Yam LYC, Lim W, Nicholls J, Yee**
585 **WKS, Yan WW, Cheung MT, Cheng VCC, Chan KH, Tsang DNC, Yung**
586 **RWH, Ng TK, Yuen KY.** 2003. Coronavirus as a possible cause of severe acute
587 respiratory syndrome. *Lancet* **361**:1319-1325.
- 588 16. **Zaki AM, van Boheemen S, Bestebroer TM, Osterhaus A, Fouchier RAM.**
589 2012. Isolation of a Novel Coronavirus from a Man with Pneumonia in Saudi
590 Arabia. *New England Journal of Medicine* **367**:1814-1820.
- 591 17. **de Groot RJ, Baker SC, Baric RS, Brown CS, Drosten C, Enjuanes L,**
592 **Fouchier RA, Galiano M, Gorbalenya AE, Memish ZA, Perlman S, Poon LL,**
593 **Snijder EJ, Stephens GM, Woo PC, Zaki AM, Zambon M, Ziebuhr J.** 2013.
594 Middle East respiratory syndrome coronavirus (MERS-CoV): announcement of
595 the Coronavirus Study Group. *J Virol* **87**:7790-7792.
- 596 18. **Li F.** 2015. Receptor recognition mechanisms of coronaviruses: a decade of
597 structural studies. *J Virol* **89**:1954-1964.
- 598 19. **Li F.** 2016. Structure, Function, and Evolution of Coronavirus Spike Proteins.
599 *Annu Rev Virol* **3**:237-261.

- 600 20. **Belouzard S, Chu VC, Whittaker GR.** 2009. Activation of the SARS
601 coronavirus spike protein via sequential proteolytic cleavage at two distinct sites.
602 Proceedings of the National Academy of Sciences of the United States of America
603 **106**:5871-5876.
- 604 21. **Millet JK, Whittaker GR.** 2014. Host cell entry of Middle East respiratory
605 syndrome coronavirus after two-step, furin-mediated activation of the spike
606 protein. Proc Natl Acad Sci U S A **111**:15214-15219.
- 607 22. **Gierer S, Bertram S, Kaup F, Wrensch F, Heurich A, Kramer-Kuhl A,
608 Welsch K, Winkler M, Meyer B, Drosten C, Dittmer U, von Hahn T,
609 Simmons G, Hofmann H, Pohlmann S.** 2013. The spike protein of the emerging
610 betacoronavirus EMC uses a novel coronavirus receptor for entry, can be
611 activated by TMPRSS2, and is targeted by neutralizing antibodies. J Virol
612 **87**:5502-5511.
- 613 23. **Shirato K, Kawase M, Matsuyama S.** 2013. Middle East respiratory syndrome
614 coronavirus infection mediated by the transmembrane serine protease TMPRSS2.
615 J Virol **87**:12552-12561.
- 616 24. **Yang Y, Du L, Liu C, Wang L, Ma C, Tang J, Baric RS, Jiang S, Li F.** 2014.
617 Receptor usage and cell entry of bat coronavirus HKU4 provide insight into bat-
618 to-human transmission of MERS coronavirus. Proc Natl Acad Sci U S A
619 **111**:12516-12521.
- 620 25. **Qian Z, Dominguez SR, Holmes KV.** 2013. Role of the spike glycoprotein of
621 human Middle East respiratory syndrome coronavirus (MERS-CoV) in virus
622 entry and syncytia formation. PLoS One **8**:e76469.
- 623 26. **Gierer S, Muller MA, Heurich A, Ritz D, Springstein BL, Karsten CB,
624 Schendzielorz A, Gnirss K, Drosten C, Pohlmann S.** 2015. Inhibition of
625 proprotein convertases abrogates processing of the middle eastern respiratory
626 syndrome coronavirus spike protein in infected cells but does not reduce viral
627 infectivity. J Infect Dis **211**:889-897.
- 628 27. **Matsuyama S, Shirato K, Kawase M, Terada Y, Kawachi K, Fukushi S,
629 Kamitani W.** 2018. Middle East Respiratory Syndrome Coronavirus Spike
630 Protein Is Not Activated Directly by Cellular Furin during Viral Entry into Target
631 Cells. J Virol **92**.

- 632 28. **Belouzard S, Madu I, Whittaker GR.** 2010. Elastase-mediated activation of the
633 severe acute respiratory syndrome coronavirus spike protein at discrete sites
634 within the S2 domain. *J Biol Chem* **285**:22758-22763.
- 635 29. **Bertram S, Glowacka I, Muller MA, Lavender H, Gnirss K, Nehlmeier I,**
636 **Niemeyer D, He Y, Simmons G, Drosten C, Soilleux EJ, Jahn O, Steffen I,**
637 **Pohlmann S.** 2011. Cleavage and activation of the severe acute respiratory
638 syndrome coronavirus spike protein by human airway trypsin-like protease. *J*
639 *Viro* **85**:13363-13372.
- 640 30. **Matsuyama S, Ujike M, Morikawa S, Tashiro M, Taguchi F.** 2005. Protease-
641 mediated enhancement of severe acute respiratory syndrome coronavirus
642 infection. *Proceedings of the National Academy of Sciences of the United States*
643 *of America* **102**:12543-12547.
- 644 31. **Kam YW, Okumura Y, Kido H, Ng LF, Bruzzone R, Altmeyer R.** 2009.
645 Cleavage of the SARS coronavirus spike glycoprotein by airway proteases
646 enhances virus entry into human bronchial epithelial cells in vitro. *PLoS One*
647 **4**:e7870.
- 648 32. **Li WD, Shi ZL, Yu M, Ren WZ, Smith C, Epstein JH, Wang HZ, Crameri G,**
649 **Hu ZH, Zhang HJ, Zhang JH, McEachern J, Field H, Daszak P, Eaton BT,**
650 **Zhang SY, Wang LF.** 2005. Bats are natural reservoirs of SARS-like
651 coronaviruses. *Science* **310**:676-679.
- 652 33. **Lau SKP, Woo PCY, Li KSM, Huang Y, Tsoi HW, Wong BHL, Wong SSY,**
653 **Leung SY, Chan KH, Yuen KY.** 2005. Severe acute respiratory syndrome
654 coronavirus-like virus in Chinese horseshoe bats. *Proceedings of the National*
655 *Academy of Sciences of the United States of America* **102**:14040-14045.
- 656 34. **Hou YX, Peng C, Yu M, Li Y, Han ZG, Li F, Wang LF, Shi ZL.** 2010.
657 Angiotensin-converting enzyme 2 (ACE2) proteins of different bat species confer
658 variable susceptibility to SARS-CoV entry. *Archives of Virology* **155**:1563-1569.
- 659 35. **Ge XY, Li JL, Yang XL, Chmura AA, Zhu G, Epstein JH, Mazet JK, Hu B,**
660 **Zhang W, Peng C, Zhang YJ, Luo CM, Tan B, Wang N, Zhu Y, Crameri G,**
661 **Zhang SY, Wang LF, Daszak P, Shi ZL.** 2013. Isolation and characterization of
662 a bat SARS-like coronavirus that uses the ACE2 receptor. *Nature* **503**:535-538.
- 663 36. **Annan A, Baldwin HJ, Corman VM, Klose SM, Owusu M, Nkrumah EE,**
664 **Badu EK, Anti P, Agbenyega O, Meyer B, Oppong S, Sarkodie YA, Kalko**

- 665 **EK, Lina PH, Godlevska EV, Reusken C, Seebens A, Gloza-Rausch F, Vallo**
666 **P, Tschapka M, Drosten C, Drexler JF.** 2013. Human betacoronavirus 2c
667 EMC/2012-related viruses in bats, Ghana and Europe. *Emerg Infect Dis* **19**:456-
668 459.
- 669 37. **Holmes KV, Dominguez SR.** 2013. The New Age of Virus Discovery: Genomic
670 Analysis of a Novel Human Betacoronavirus Isolated from a Fatal Case of
671 Pneumonia. *Mbio* **4**.
- 672 38. **Lau SK, Li KS, Tsang AK, Lam CS, Ahmed S, Chen H, Chan KH, Woo PC,**
673 **Yuen KY.** 2013. Genetic characterization of Betacoronavirus lineage C viruses in
674 bats reveals marked sequence divergence in the spike protein of pipistrellus bat
675 coronavirus HKU5 in Japanese pipistrelle: implications for the origin of the novel
676 Middle East respiratory syndrome coronavirus. *J Virol* **87**:8638-8650.
- 677 39. **Li WH, Moore MJ, Vasilieva N, Sui JH, Wong SK, Berne MA,**
678 **Somasundaran M, Sullivan JL, Luzuriaga K, Greenough TC, Choe H,**
679 **Farzan M.** 2003. Angiotensin-converting enzyme 2 is a functional receptor for
680 the SARS coronavirus. *Nature* **426**:450-454.
- 681 40. **Raj VS, Mou HH, Smits SL, Dekkers DHW, Muller MA, Dijkman R, Muth**
682 **D, Demmers JAA, Zaki A, Fouchier RAM, Thiel V, Drosten C, Rottier PJM,**
683 **Osterhaus A, Bosch BJ, Haagmans BL.** 2013. Dipeptidyl peptidase 4 is a
684 functional receptor for the emerging human coronavirus-EMC. *Nature* **495**:251-
685 254.
- 686 41. **Wang Q, Qi J, Yuan Y, Xuan Y, Han P, Wan Y, Ji W, Li Y, Wu Y, Wang J,**
687 **Iwamoto A, Woo PC, Yuen KY, Yan J, Lu G, Gao GF.** 2014. Bat origins of
688 MERS-CoV supported by bat coronavirus HKU4 usage of human receptor CD26.
689 *Cell Host Microbe* **16**:328-337.
- 690 42. **Luo CM, Wang N, Yang XL, Liu HZ, Zhang W, Li B, Hu B, Peng C, Geng**
691 **QB, Zhu GJ, Li F, Shi ZL.** 2018. Discovery of novel bat coronaviruses in south
692 China that use the same receptor as MERS coronavirus. *J Virol*
693 doi:10.1128/jvi.00116-18.
- 694 43. **Lau SKP, Zhang L, Luk HKH, Xiong L, Peng X, Li KSM, He X, Zhao PS,**
695 **Fan RYY, Wong ACP, Ahmed SS, Cai JP, Chan JFW, Sun Y, Jin D, Chen H,**
696 **Lau TCK, Kok RKH, Li W, Yuen KY, Woo PCY.** 2018. Receptor Usage of a
697 Novel Bat Lineage C Betacoronavirus Reveals Evolution of Middle East

- 698 Respiratory Syndrome-Related Coronavirus Spike Proteins for Human Dipeptidyl
699 Peptidase 4 Binding. *J Infect Dis* **218**:197-207.
- 700 44. **Yang Y, Liu C, Du L, Jiang S, Shi Z, Baric RS, Li F.** 2015. Two Mutations
701 Were Critical for Bat-to-Human Transmission of Middle East Respiratory
702 Syndrome Coronavirus. *J Virol* **89**:9119-9123.
- 703 45. **Park JE, Li K, Barlan A, Fehr AR, Perlman S, McCray PB, Jr., Gallagher T.**
704 2016. Proteolytic processing of Middle East respiratory syndrome coronavirus
705 spikes expands virus tropism. *Proc Natl Acad Sci U S A* **113**:12262-12267.
- 706 46. **Hofmann H, Hattermann K, Marzi A, Gramberg T, Geier M, Krumbiegel**
707 **M, Kuate S, Uberla K, Niedrig M, Pohlmann S.** 2004. S protein of severe acute
708 respiratory syndrome-associated coronavirus mediates entry into hepatoma cell
709 lines and is targeted by neutralizing antibodies in infected patients. *Journal of*
710 *Virology* **78**:6134-6142.
- 711 47. **Gillim-Ross L, Taylor J, Scholl DR, Ridenour J, Masters PS, Wentworth DE.**
712 2004. Discovery of novel human and animal cells infected by the severe acute
713 respiratory syndrome coronavirus by replication-specific multiplex reverse
714 transcription-PCR. *J Clin Microbiol* **42**:3196-3206.
- 715 48. **Cai Y, Yu SQ, Postnikova EN, Mazur S, Bernbaum JG, Burk R, Zhang T,**
716 **Radoshitzky SR, Muller MA, Jordan I, Bollinger L, Hensley LE, Jahrling**
717 **PB, Kuhn JH.** 2014. CD26/DPP4 cell-surface expression in bat cells correlates
718 with bat cell susceptibility to Middle East respiratory syndrome coronavirus
719 (MERS-CoV) infection and evolution of persistent infection. *PLoS One*
720 **9**:e112060.
- 721 49. **Xu X, Yuan X, Li N, Dewey WL, Li PL, Zhang F.** 2016. Lysosomal cholesterol
722 accumulation in macrophages leading to coronary atherosclerosis in CD38(-/-)
723 mice. *J Cell Mol Med* **20**:1001-1013.
- 724 50. **Liu C, Ma Y, Yang Y, Zheng Y, Shang J, Zhou Y, Jiang S, Du L, Li J, Li F.**
725 2016. Cell Entry of Porcine Epidemic Diarrhea Coronavirus Is Activated by
726 Lysosomal Proteases. *J Biol Chem* **291**:24779-24786.
- 727 51. **Lambeir AM, Durinx C, Scharpe S, De Meester I.** 2003. Dipeptidyl-peptidase
728 IV from bench to bedside: an update on structural properties, functions, and
729 clinical aspects of the enzyme DPP IV. *Crit Rev Clin Lab Sci* **40**:209-294.

- 730 52. **Clarke NE, Turner AJ.** 2012. Angiotensin-converting enzyme 2: the first
731 decade. *Int J Hypertens* **2012**:307315.
- 732 53. **Ou X, Zheng W, Shan Y, Mu Z, Dominguez SR, Holmes KV, Qian Z.** 2016.
733 Identification of the Fusion Peptide-Containing Region in Betacoronavirus Spike
734 Glycoproteins. *J Virol* **90**:5586-5600.
735
736

737 **Figure legends**

738 **Figure 1.** Screening for cells lines that are suitable for studying lysosomal-proteases-
739 activated coronavirus entry. To screen for cell lines that endogenously express no or low
740 level of receptor protein for the coronavirus of interest, MERS-CoV pseudoviruses (A) or
741 SARS-CoV pseudoviruses (B) were used to enter a number of cells from different tissues
742 of different host species (human, monkey, and bat). Entry efficiency was characterized by
743 luciferase activity accompanying entry, and calibrated against the highest entry efficiency
744 (i.e., MERS-CoV entry into MRC5 cells was taken as 100% in panel A, whereas SARS-
745 CoV entry into Vero cells was taken as 100% in panel B). Mock: no pseudoviruses were
746 added. Error bars indicate S.E.M. (n=5). (C) To screen for cell lines that can be easily
747 transfected and hence controlled to exogenously express receptor protein for the
748 coronavirus of interest, different cells were transfected with a plasmid encoding human
749 DPP4; subsequently, the expression level of human DPP4 in each of the cell lines was
750 detected through Western blotting analysis using an antibody recognizing its C-terminal
751 C9 tag. The expression level of β -actin in each of the cell lines was used as positive
752 controls. (D) MTT cell viability assay showing that the viabilities of three types of cells
753 were not affected by the presence of different protease inhibitors. Error bars indicate
754 S.E.M. (n=5). There is no statistical significance for each cell group (i.e., $P>0.05$ based
755 on two-tailed t test).

756

757 **Figure 2.** Roles of lysosomal proteases in MERS-CoV-spike-mediated membrane fusion.

758 (A) Roles of lysosomal proteases in MERS-CoV pseudovirus entry. Three types of cells,
759 human HEK293T (h-HEK293T), human HeLa (h-HeLa) and bat Tb1-Lu (b-Tb1-Lu),

760 were controlled to exogenously express human DPP4 as described in Fig. 1C, and then
761 subjected to MERS-CoV pseudovirus entry as described in Fig. 1A. Furin inhibitor
762 chloromethylketone, cell-surface protease (i.e., TMPRSS2) inhibitor camostat, or
763 lysosomal protease (i.e., cathepsins) inhibitor E64d was used in parallel experiments to
764 investigate the relative contributions of different proteases to MERS-CoV pseudovirus
765 entry. The expression levels of cell surface-associated C9-tagged human DPP4 were
766 measured through Western blot analysis using an anti-C9 tag monoclonal antibody, and
767 were further calibrated across the three types of cells. (B) MERS-CoV-spike-mediated
768 cell-cell fusion in the presence of lysosomal extracts. h-HEK293T cells exogenously
769 expressing MERS-CoV spike and h-HEK293T cells exogenously expressing human
770 DPP4 were mixed together at pH 5.6 in the presence of lysosomal extracts from h-
771 HEK293T cells, h-HeLa cells, b-Tb1-Lu cells, or bat BKD9 (b-BKD9) cells. Cell-cell
772 fusion efficiency was characterized by luciferase activity accompanying fusion, and
773 calibrated against the highest fusion efficiency (i.e., in the presence of lysosomal extracts
774 from b-Tb1-Lu cells). Three negative controls were used: (i) cells not expressing human
775 DPP4 were used for fusion (i.e., no receptor); (ii) no lysosomal proteases were added to
776 the medium and the medium was at neutral pH (i.e., no treatment); (iii) no lysosomal
777 proteases were added, but the medium was at pH 5.6 (i.e., low pH treatment). For both
778 panels, statistic analyses were performed using two-tailed *t*-test. Error bars indicate
779 S.E.M. (n=4). *** $P < 0.001$. ** $P < 0.01$.

780

781 **Figure 3.** Characterization of the purity of lysosomal extracts from different cell lines.

782 Because alkaline phosphatase (ALP) and cytochrome P450 reductase (CPR) are

783 enzymatic markers of plasma and endoplasmic reticulum (ER), respectively, the purified
784 lysosomal extracts and whole cell lysates from different cell lines (for each cell line,
785 lysosomal extracts and whole cell lysates were in equal concentrations) were assayed for
786 their ALP activities (panel A) and CPR activities (panel B) as evaluation of potential
787 contaminants from other cell organelles. Error bars indicate S.E.M. (n=3) (some of the
788 error bars may be too small to be seen).

789

790 **Figure 4.** Roles of lysosomal proteases in SARS-CoV-spike-mediated membrane fusion.

791 The experiments were performed in the same way as in Fig. 2, except that SARS-CoV
792 spike and its receptor human ACE2 replaced MERS-CoV spike and human DPP4,
793 respectively.

794

795 **Figure 5.** Cleavage of cell-surface-expressed MERS-CoV spike using purified lysosomal

796 extracts. (A) Cleavage of cell-surface-expressed MERS-CoV spike using lysosomal
797 extracts from a number of cell lines. MERS-CoV spike was exogenously expressed on
798 the surface of h-HEK293T cells, and then treated with 50 $\mu\text{g/ml}$ lysosomal extracts (from
799 different types of cells) at pH 5.6 for 30 minutes. The cleavage state of MERS-CoV spike
800 was detected through Western blotting analysis using an antibody recognizing its C-
801 terminal C9 tag. (B) Cleavage of cell-surface-expressed MERS-CoV spike using 100
802 $\mu\text{g/ml}$ lysosomal extracts (from two types of cells) at pH 5.6 in a time-dependent manner
803 (i.e., 10, 30, and 60 minutes). These experiments were repeated five times, and
804 representative results are shown here.

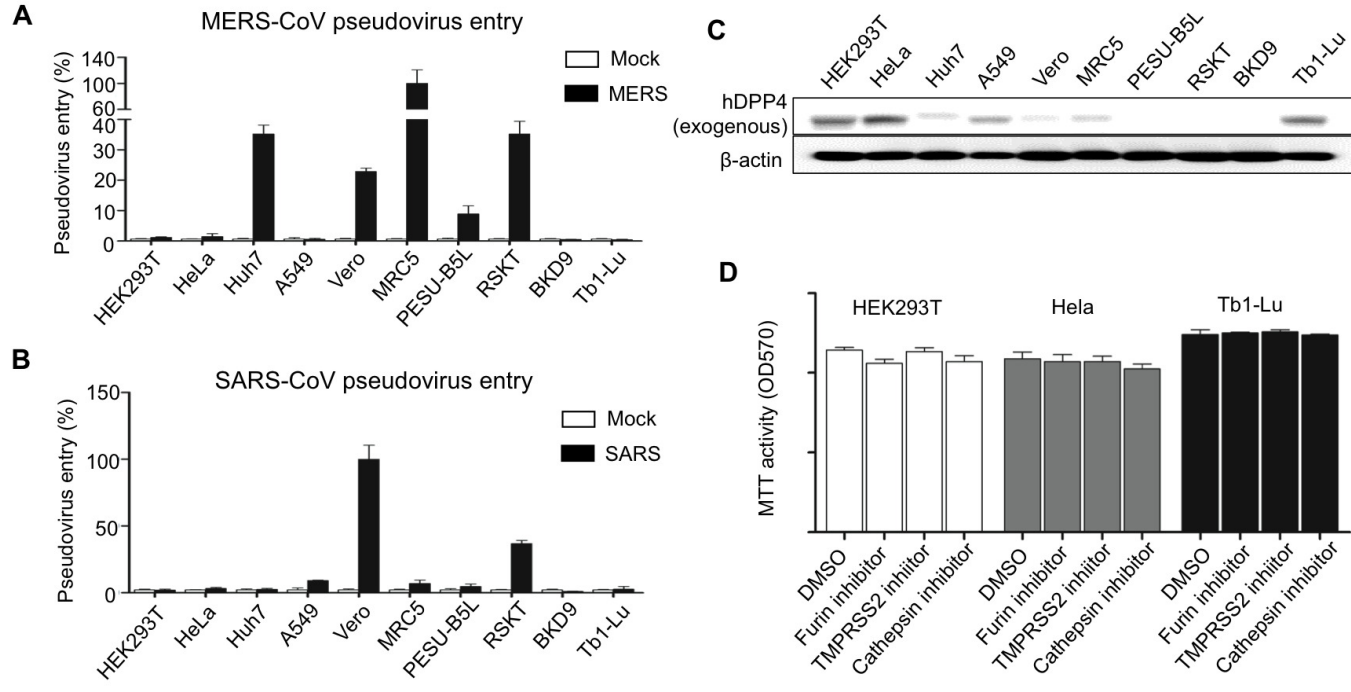
805

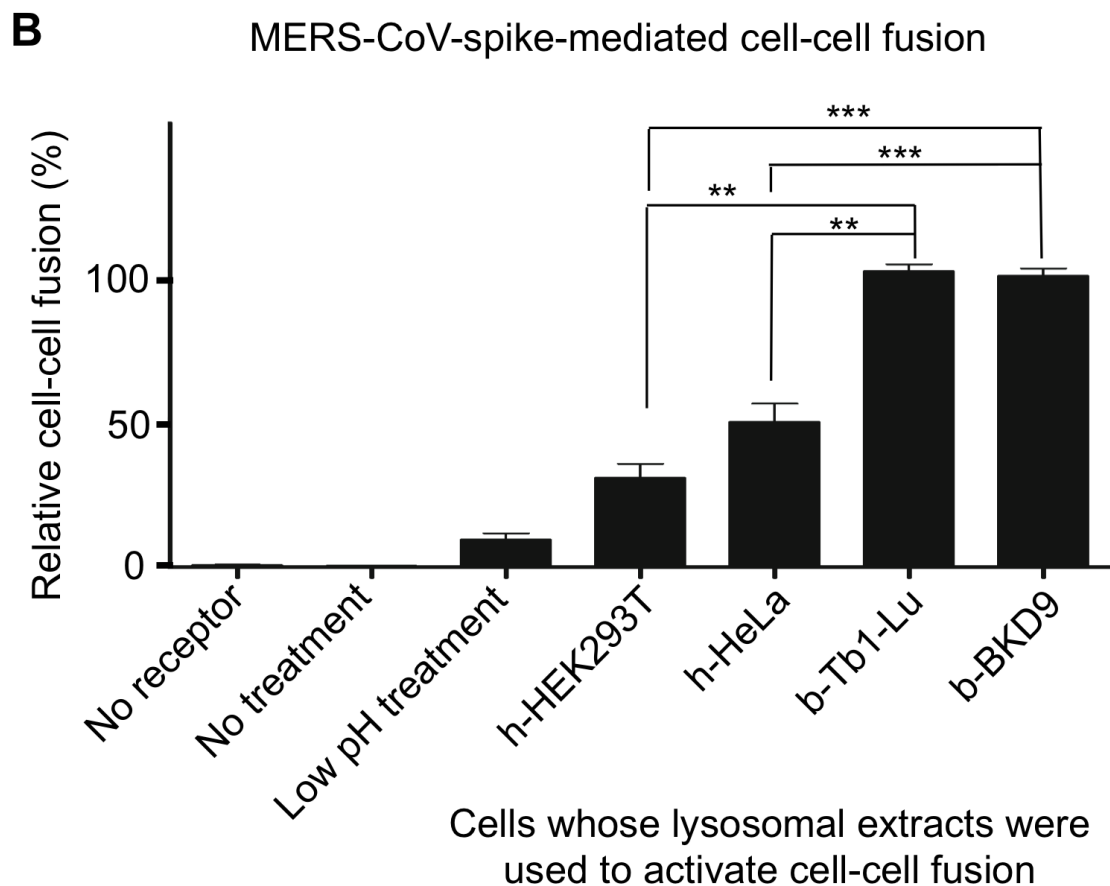
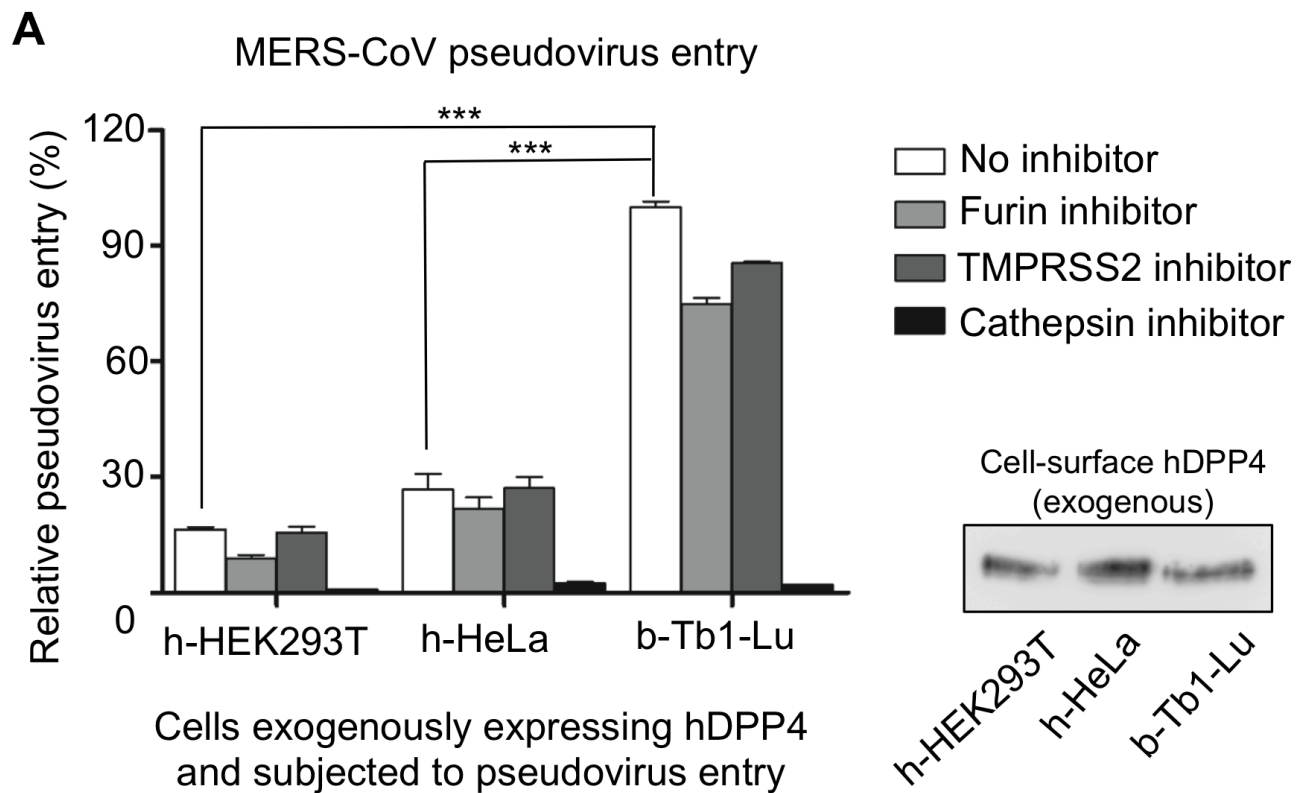
806 **Figure 6.** Cleavage of cell-surface-expressed HKU4 spike using purified lysosomal
807 extracts. The experiments were performed in the same way as in Fig. 5A, except that
808 HKU4 spike (either wild type or containing an N762 mutation that removed a
809 glycosylation site from the lysosomal protease motif) replaced MERS-CoV spike. These
810 experiments were repeated five times, and representative results are shown here.

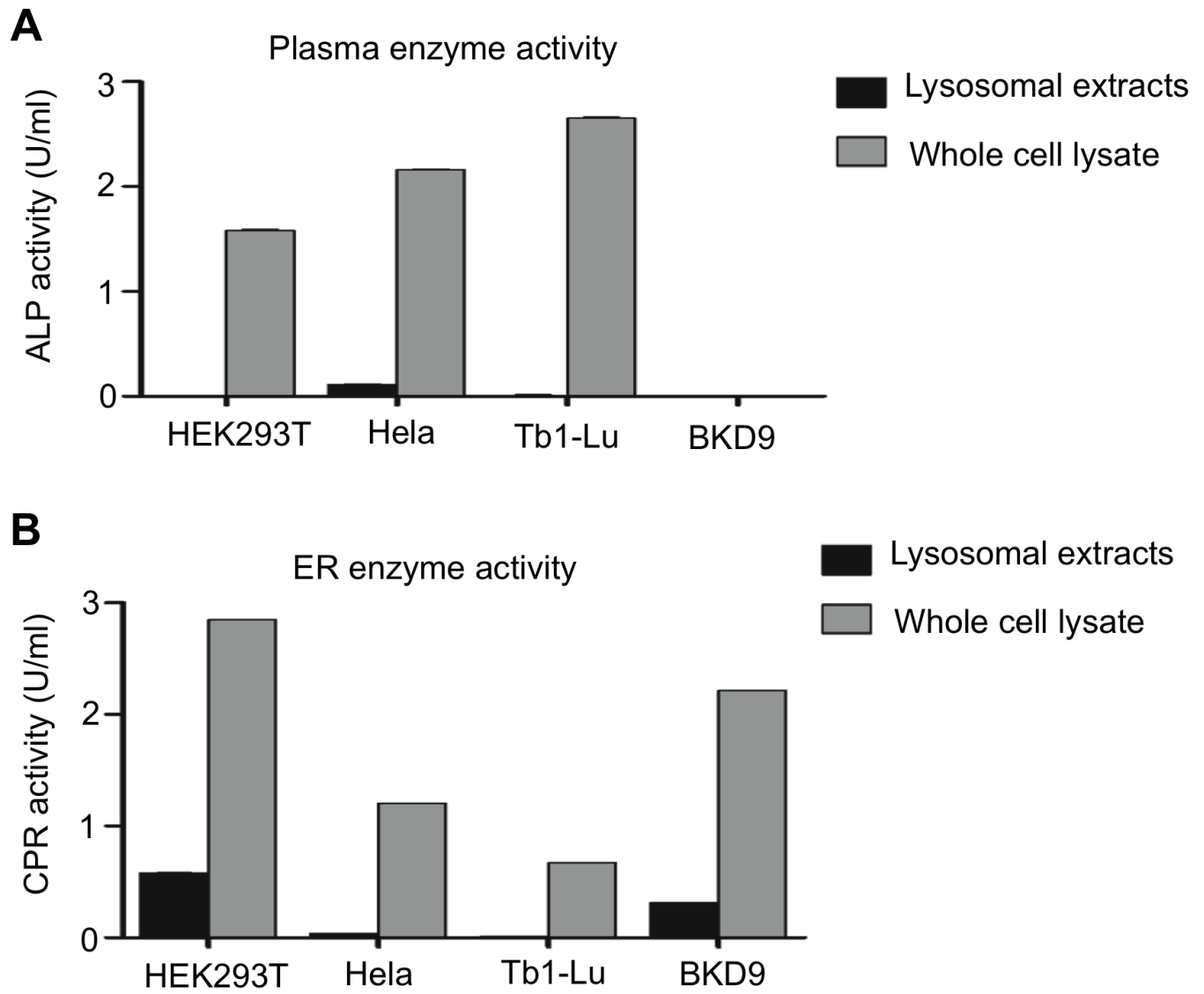
811

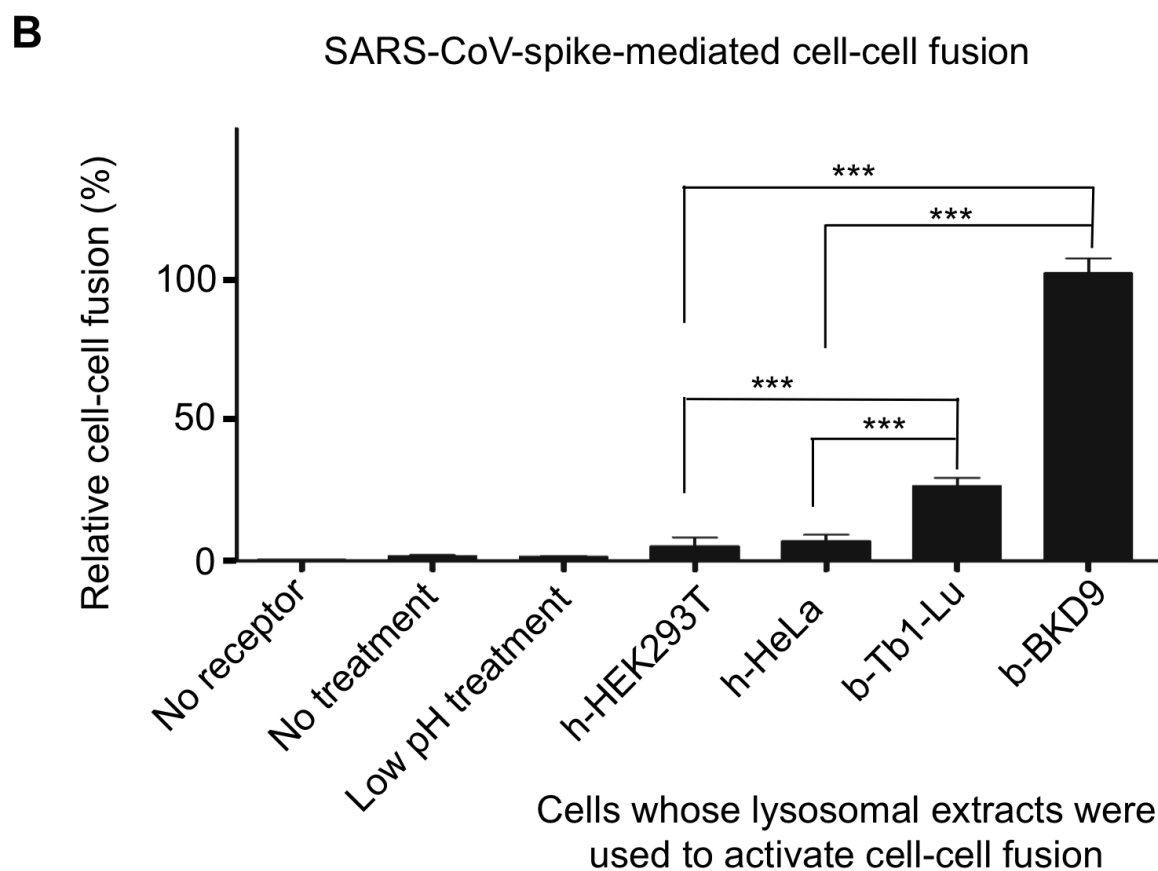
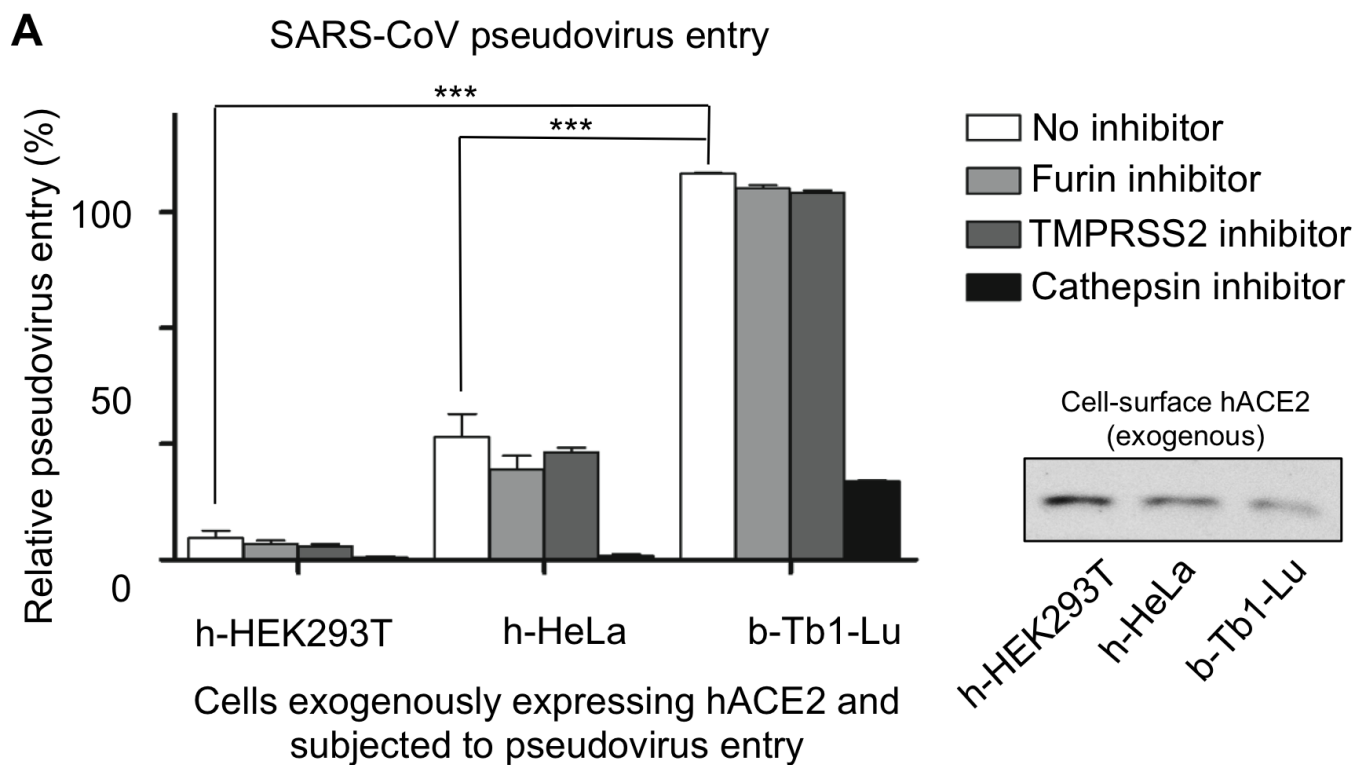
812

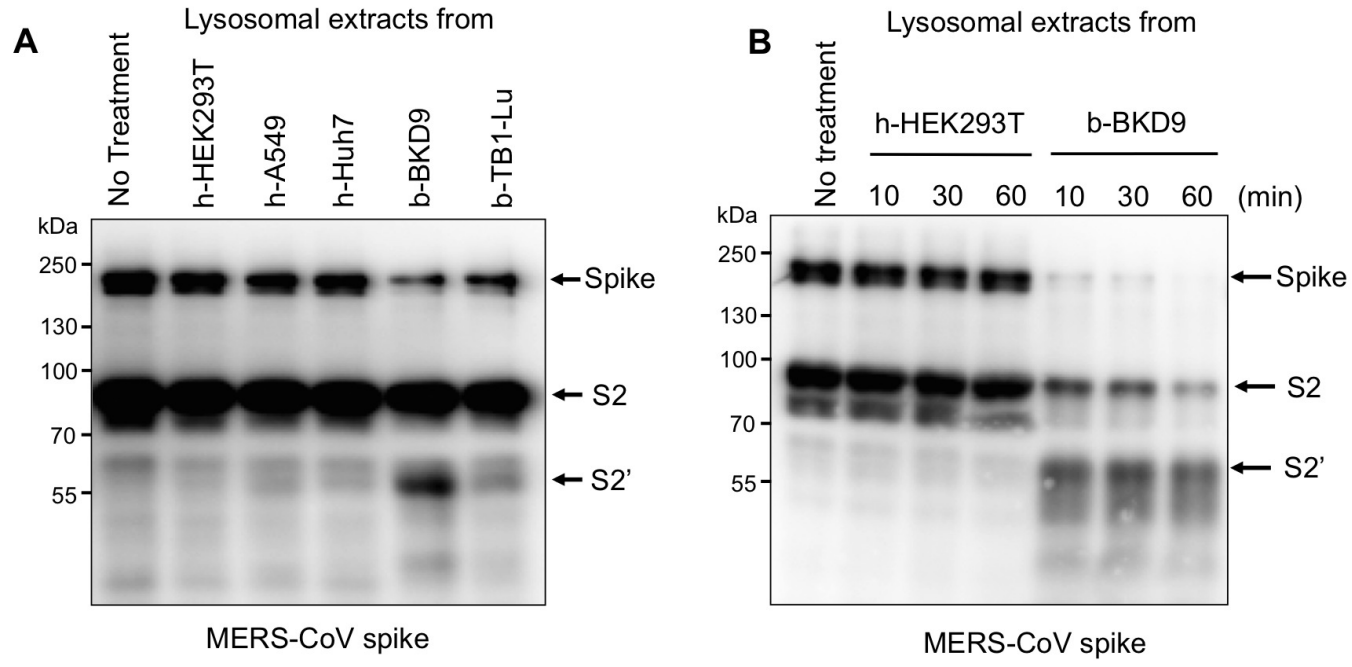
813

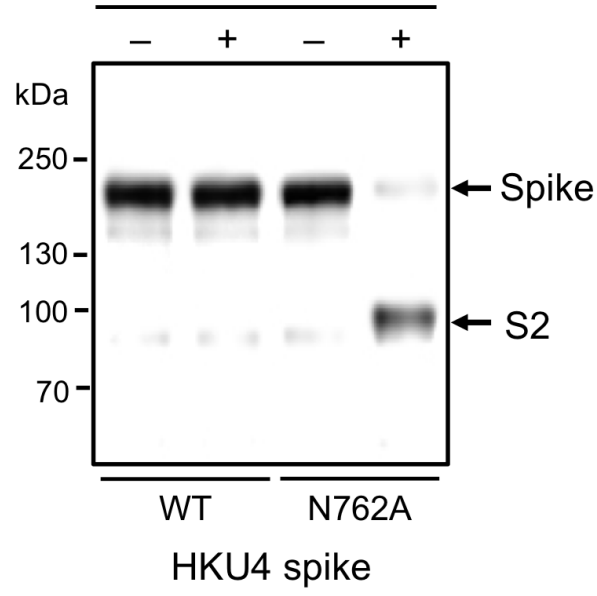










A Lysosomal extracts from
h-HEK293T**B** Lysosomal extracts from
b-Tb1-Lu